

# Solar neutrinos: global analysis and implications for SNO

---

**John N. Bahcall\***

*School of Natural Sciences, Institute for Advanced Study, Princeton, NJ 08540*

**Plamen I. Krastev†**

*School of Natural Sciences, Institute for Advanced Study, Princeton, NJ 08540,  
Dept. of Physics and Astronomy, University of Delaware, Newark, DE 19716*

**Alexei Yu. Smirnov‡**

*International Center for Theoretical Physics, 34100 Trieste, Italy*

**ABSTRACT:** We present a global analysis of all the available solar neutrino data treating consistently the  ${}^8\text{B}$  and *hep* neutrino fluxes as free parameters. The analysis reveals at 99.7% C.L. eight currently-allowed discrete regions in two-neutrino oscillation space, five regions corresponding to active neutrinos and three corresponding to sterile neutrinos. Most of the allowed oscillation solutions are robust with respect to changes in the analysis procedures, but the traditional vacuum solution is fragile. The globally-permitted range of the  ${}^8\text{B}$  neutrino flux, 0.45 to 1.95 in units of the BP2000 flux, is comparable to the  $3\sigma$  range allowed by the standard solar model. We discuss the implications for SNO of a low mass,  $\Delta m^2 \sim 6 \times 10^{-12} \text{ eV}^2$ , vacuum oscillation solution, previously found by Raghavan, and by Krastev and Petcov, but absent in recent analyses that included Super-Kamiokande data. For the SNO experiment, we present refined predictions for the charged-current rate and the ratio of the neutral-current rate to charged-current rate. The predicted charged-current rate can be clearly distinguished from the no-oscillation rate only for the LMA solution. The predicted ratio of the neutral-current rate to charged-current rate is distinguishable from the no-oscillation ratio for the LMA, SMA, LOW, and VAC solutions for active neutrinos.

**KEYWORDS:** solar and atmospheric neutrinos, neutrino and gamma astronomy, neutrino physics.

---

\*E-mail address: jnb@ias.edu

†E-mail address: krastev@ias.edu

‡E-mail address: smirnov@ictp.trieste.it

---

## Contents

<b>1. Introduction</b>	<b>1</b>
<b>2. Global solutions</b>	<b>4</b>
2.1 Results	4
2.2 Computational method	8
<b>3. Variations on a theme</b>	<b>11</b>
<b>4. Just <math>\text{So}^2</math> Solution</b>	<b>13</b>
<b>5. Implications for the SNO experiment</b>	<b>16</b>
5.1 Predictions for the charged-current rate	17
5.2 The ratio of neutral-current rate to charged-current rate	18
<b>6. Discussion</b>	<b>20</b>

---

## 1. Introduction

From the inception of the subject, solar neutrino research has been motivated by two apparently conflicting goals: 1) to test the theory of nuclear fusion reactions in stars; and 2) to determine neutrino characteristics. In the approximately four decades since its inception, the subject has been dramatically transformed. In the first paper reporting an experimental result [1], the measurement was compared only with the then existing standard solar model [2]. In the ensuing decades, the emphasis gradually shifted to particle physics as enormous progress was made both experimentally and theoretically. New experiments were reported <sup>2</sup>, including the results of Kamiokande [3], SAGE [4], GALLEX [5], Super-Kamiokande [6], GNO [7], refined results of the chlorine experiment [8], and (in the near future) there will be

---

<sup>2</sup>The total rates in the Homestake (chlorine), Kamiokande, SAGE, GALLEX + GNO, and Super-Kamiokande experiments cannot be fit well without some form of new physics even if the solar neutrino fluxes are allowed to be free parameters. Allowing the  $p-p$ ,  ${}^7\text{Be}$ ,  ${}^8\text{B}$ ,  ${}^{13}\text{N}$ , and  ${}^{15}\text{O}$  fluxes to be free parameters, the minimum  $\chi^2$  is obtained for zero fluxes of  ${}^7\text{Be} = {}^{13}\text{N} = {}^{15}\text{O} = 0.0$  and even this unphysical solution is acceptable only at the 99.6% C.L. This result has been stable for many years as experimental results have been refined.

results from SNO [9], BOREXINO [10], KamLAND [11] and ICARUS [12]. In parallel activities, the theories of vacuum [13] and matter-induced (MSW) [14] neutrino oscillations were developed and explored and the solar models were refined [15] and verified by helioseismology [16].

In the last decade or so, it has become customary to blur the distinction between the two goals of solar neutrino research, measuring neutrino properties and using neutrinos to learn about stars. The results of all the experiments are combined in a statistical analysis from which the allowed ranges of neutrino masses and mixing angles are extracted, including among the input data the calculated standard solar model neutrino fluxes and their associated uncertainties.

In the present paper, we take a modest step toward separating the two subjects, neutrino physics and neutrino astronomy, of solar neutrino research. We allow the important  $^8\text{B}$  neutrino flux, and the much less important *hep* flux, to be free parameters and perform a systematic global analysis [17, 18] of all the available solar neutrino data (for early work allowing the  $^8\text{B}$  neutrino flux to vary freely, see ref. [19] and for related work, see refs. [17, 20, 21, 22]). We extract from the analysis the allowed ranges of the  $^8\text{B}$  and *hep* fluxes as well as the neutrino parameters,  $\Delta m^2$  and  $\tan^2 \theta$ . We continue, following what is currently common practice, to constrain the other solar neutrino fluxes with the aid of the calculated fluxes and uncertainties given by the BP2000 standard solar model [23].

We emphasize the robustness of most of the allowed regions, and the fragility of some regions, to small changes in the data analysis. We illustrate the effects of changes in the analysis by performing the global analysis of all the data in different ways. In particular, we demonstrate the effects of the common practices (of which we have also been guilty) of treating the  $^8\text{B}$  absolute flux differently between the measured rates and the measured spectral data and the effects of double counting of the SuperKamiokande rate.

We have also carried out solutions in which the  $^7\text{Be}$ ,  $^8\text{B}$ , and *hep* fluxes are all allowed to vary without taking into account the solar model predictions, but in this case the range of solutions is too large at present to be useful to discuss. The situation will presumably change when data from the SNO, KamLAND, BOREXINO and ICARUS experiments are available. In a work in preparation, we will report on the implications of the global solutions found here for  $^7\text{Be}$  experiments like BOREXINO.

In Section 2, we present the global solutions for both active and sterile neutrinos when the  $^8\text{B}$  and *hep* fluxes are treated as free parameters. Section 3 shows that some solutions (LMA, SMA, and LOW) are robust with respect to changes in the analysis constraints while other solutions (vacuum solutions) are more fragile. We discuss in Section 4 the characteristics of the Just So<sup>2</sup> solution and in Section 5 we present the predictions of the currently-allowed oscillation solutions for the measurements with SNO of the charged-current rate and the (charged-current rate) / (neutral-current rate) ratio. We summarize and discuss our main results in Section 6.

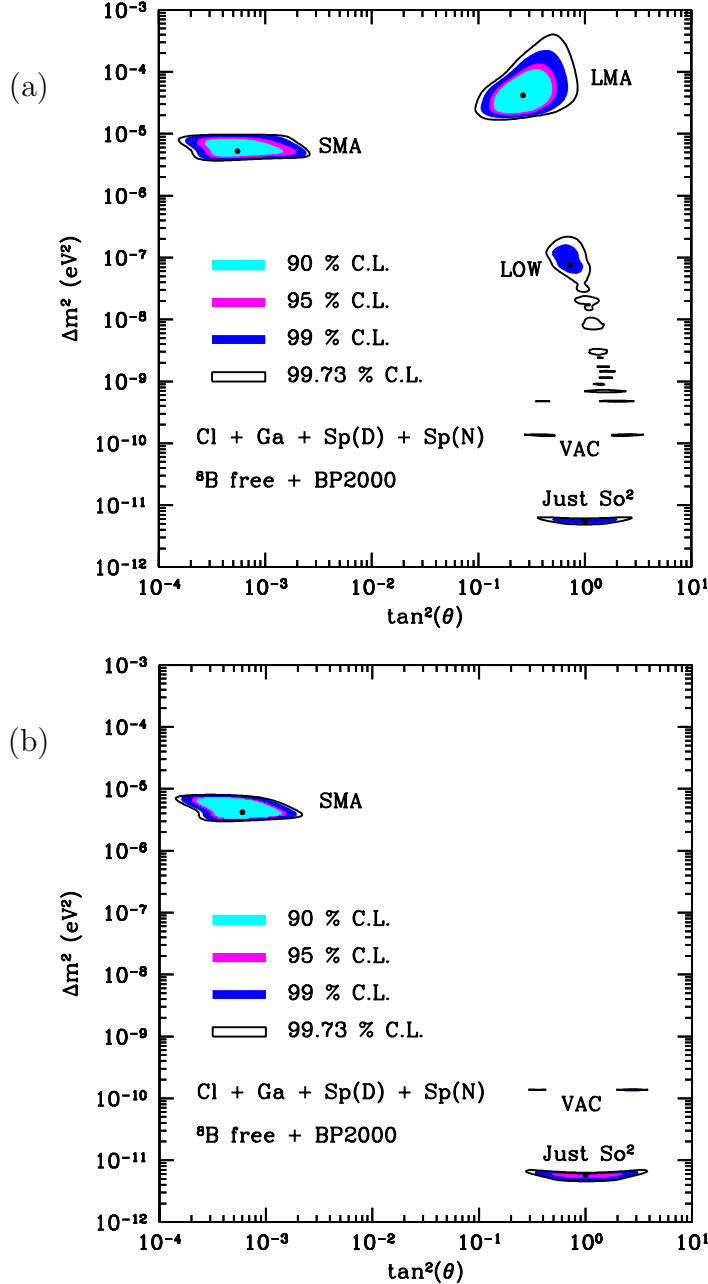


**Figure 1:** Global solutions, free <sup>8</sup>B and *hep* fluxes. (a) Active neutrinos. (b) Sterile neutrinos. The input data include the total rates measured in the Homestake, SAGE, and GALLEX + GNO experiments and the electron recoil energy spectrum measured by Super-Kamiokande during the day and also the spectrum measured at night. The best-fit points are marked by dark circles; the allowed regions are shown at 90%, 95%, 99%, and 99.73% C.L. .

## 2. Global solutions

We summarize our main results on the global two-neutrino oscillation solutions in Section 2.1 and describe in Section 2.2, which is intended for aficionados only, our calculational procedures.

### 2.1 Results

Figure 1 shows the globally allowed solutions for both active, Figure 1a, and sterile neutrinos, Figure 1b. The results are presented at four different confidence levels ranging from 90% to 99.73% (corresponding to  $3\sigma$ ). There are five isolated regions of allowed solutions for active neutrinos (LMA, SMA, LOW, VAC, and Just So<sup>2</sup>) and three separate solutions for sterile neutrinos (SMA, VAC, and Just So<sup>2</sup>).

The allowed oscillation regions are shown for a global solution with the <sup>8</sup>B neutrino flux treated as a free parameter in all of the analysis. The allowed regions at different confidence levels are presented for neutrino oscillation models that fit the total rates measured in the chlorine [8] and gallium [4, 5, 7] solar neutrinos experiments, as well as the electron recoil energy spectrum measured by the Super-Kamiokande collaboration [6] during the day and the spectrum measured at night. We treat as one experiment the combined results of the GALLEX and GNO measurements and consider the SAGE results to be an independent experiment. We do not include in this analysis the Super-Kamiokande total rate, since to a large extent the total rate is represented by the flux in each of the spectral energy bins. However, since many groups analyzing solar neutrino data include both the total Super-Kamiokande rate and the spectral data, we perform the analysis in this way in the following section, Section 3.

The best-fit points in each region are shown as black dots. The measurements and errors are taken from the publications of the experimental groups. We use in this paper solar neutrino data that appeared in papers published before February 1, 2001 or in Neutrino 2000. The theoretical errors on all the other fluxes are taken from the BP2000 solar model [23]. The Super-Kamiokande measurement for the <sup>8</sup>B neutrino flux is  $\phi(^8B) = (2.40 \pm 0.03_{-0.07}^{+0.08}) \times 10^6 \text{cm}^{-2} \text{s}^{-1}$ .

Matter effects are significant for all of the allowed islands of solution space between  $10^{-9} \text{eV}^2 \leq \Delta m^2 \leq 3 \times 10^{-7} \text{eV}^2$ . We call this collection of islands the LOW solution. In some ways of analyzing the data, all of the LOW islands are surrounded by a single  $3\sigma$  contour.

Following Fogli, Lisi, and Montanino [24] and de Gouvea, Friedland, and Murayama [21], we have given our results in terms of  $\tan^2 \theta$  rather than  $\sin^2 2\theta$  in order to include solutions with mixing angles greater than  $\pi/4$  (the so-called ‘dark side’). The general procedure that we have used in deriving the allowed regions is described in ref. [17]; see Section 2.2 for some details.

Solution	$\Delta m^2$	$\tan^2(\theta)$	$\chi_{\min}^2$	g.o.f.
LMA	$4.2 \times 10^{-5}$	$2.6 \times 10^{-1}$	29.0	75%
SMA	$5.2 \times 10^{-6}$	$5.5 \times 10^{-4}$	31.1	66%
LOW	$7.6 \times 10^{-8}$	$7.2 \times 10^{-1}$	36.0	42%
Just So <sup>2</sup>	$5.5 \times 10^{-12}$	$1.0 \times 10^0$	36.1	42%
VAC	$1.4 \times 10^{-10}$	$3.8 \times 10^{-1}$	37.5	36%
Sterile SMA	$4.2 \times 10^{-6}$	$6.0 \times 10^{-4}$	32.5	59%
Sterile Just So <sup>2</sup>	$5.5 \times 10^{-12}$	$1.0 \times 10^0$	36.5	40%
Sterile VAC	$1.4 \times 10^{-10}$	$3.6 \times 10^{-1}$	41.4	21%

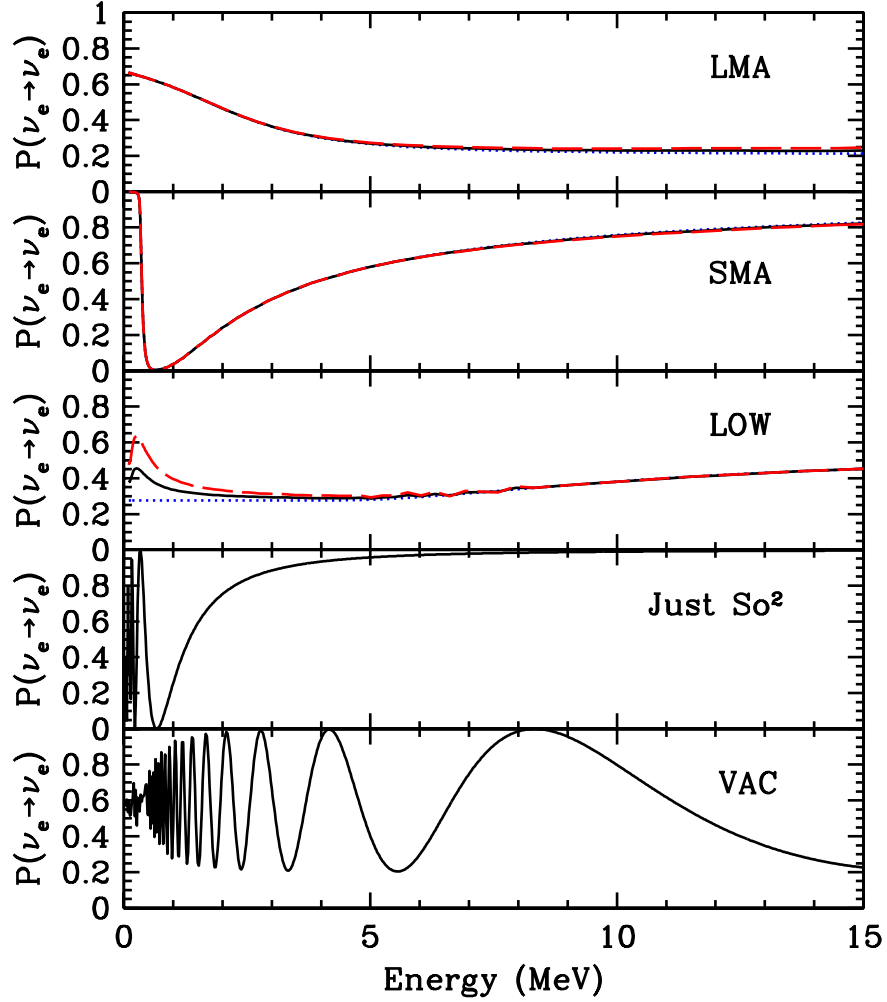
**Table 1: Best-fit global oscillation parameters.** The oscillation solutions are obtained by varying the  ${}^8\text{B}$  and  $hep$  fluxes as free parameters in a consistent way: simultaneously in the rates and in the night and day spectrum fits. The first five rows refer to active neutrinos (see Figure 1a) and the last three rows refer to sterile neutrinos (see Figure 1b). The differences of the squared masses are given in  $\text{eV}^2$ . The number of degrees of freedom is 35 [36(spectrum) + 3(rates) - 4(parameters:  $\Delta m^2$ ,  $\theta$ , and the  ${}^8\text{B}$  and  $hep$  fluxes)].

Table 1 summarizes the properties of the best-fit points of each allowed region:  $\Delta m^2$ ,  $\tan^2 \theta$ , and goodness of fit,  $\text{g.o.f.} = 1 - \text{C.L.}$  All of the solutions listed in Table 1 and shown in Figure 1 are allowed at a comfortable confidence level. The LMA and the SMA solutions are slightly preferred.

The global minimum,  $\chi_{\min}^2/\text{d.o.f.} = 29.0/35 = 0.83$ , found here (see Table 1) is somewhat smaller than would be expected for data that have a true  $\chi^2$  distribution with correctly estimated errors. The principal reason that the  $\chi^2$  is somewhat small is that the Super-Kamiokande day and night recoil energy spectra are very well fit by undistorted  ${}^8\text{B}$  and  $hep$  energy spectra,  $\chi_{\min}^2 = 29.0$  for 34 d.o.f., with  $\phi({}^8\text{B}) = 0.46\phi({}^8\text{B})_{\text{BP2000}}$  and  $\phi(hep) = 1.0\phi(hep)_{\text{BP2000}}$  and C.L. of 29% .

Figure 2 shows the computed survival probabilities for electron-type neutrinos as a function of energy for the day (no regeneration in the earth), the night (with regeneration), and the annual average. The probabilities were calculated for the best-fit parameters listed in Table 1. The two most striking aspects of this figure are the smallness of the day-night difference (clearly visible in the figure only for the LOW solution at energies below 1 MeV) and the relative flatness (except for the fragile VAC solution, see Section 3) of the survival probabilities at higher energies.

Most previous global analyses (including some analyses that we have published) that took account of Super-Kamiokande data on the recoil energy spectrum and the day-night effect have treated the  ${}^8\text{B}$  absolute flux differently in fitting the spectral data and in fitting the total rate. In previous analyses, the  ${}^8\text{B}$  neutrino flux was treated as a free parameter in fitting the Super-Kamiokande spectral data but was treated as an input parameter, constrained by the calculated standard solar model



**Figure 2:** Survival probabilities. The figure presents the yearly-averaged, best-fit survival probabilities for an electron neutrino that is created in the sun to remain an electron neutrino upon arrival at the earth. The survival probabilities for the sterile solutions, SMA, Just  $\text{So}^2$ , and SMA, are very similar to their counterparts for active neutrinos and are not plotted here. The full line refers to the average survival probabilities computed taking into account regeneration in the earth and the dotted line refers to calculations for the daytime that do not include regeneration. The dashed line includes regeneration at night. There are only slight differences between the computed regeneration probabilities for the detectors located at the positions of Super-Kamiokande, SNO and the Gran Sasso Underground Laboratory (see ref. [25]).

uncertainties, in fitting the data for the measured total rates of the chlorine, gallium, and electron scattering experiments. This lack of consistency was not present when only rate data were fitted.

Solution	$^8\text{B}$ (bf)	$^8\text{B}$ (min)	$^8\text{B}$ (max)	$hep$ (bf)	$hep$ (min)	$hep$ (max)
LMA	1.31	0.78	1.95	0.5	0.0	8.5
SMA	0.61	0.50	1.42	1.0	0.0	5.5
LOW	0.87	0.74	1.08	0.75	0.0	3.5
Just $\text{So}^2$	0.47	0.45	0.48	0.5	0.0	2.0
VAC	0.55	0.53	0.81	0.25	0.0	4.0
Sterile SMA	0.62	0.49	1.25	1.0	0.0	5.5
Sterile Just $\text{So}^2$	0.47	0.44	0.49	0.5	0.0	2.5
Sterile VAC	0.57	0.54	0.60	1.0	0.0	12.0

**Table 2: Ranges of allowed fluxes.** The table lists the minimum (min) and maximum (max) values that are allowed at 99.73% C.L. for the  $^8\text{B}$  and  $hep$  fluxes as well as the best fit (bf) values within each of the allowed regions. The  $^8\text{B}$  and  $hep$  fluxes were allowed to vary freely and consistently; the other neutrino fluxes are constrained by the errors given in the BP2000 solar model predictions. The first five rows refer to active neutrinos (see Figure 1a) and the last three rows refer to sterile neutrinos (see Figure 1b). The best-fit global solutions are shown as black dots in Figure 1a and Figure 1b.

Table 2 shows, for each allowed oscillation region, the total range of the  $^8\text{B}$  and  $hep$  fluxes permitted at 99.73% C.L. . The allowed regions were identified in a search in which  $\Delta m^2$ ,  $\tan^2 \theta$ , and the  $^8\text{B}$  and  $hep$  fluxes were all varied freely. The tabulated values represent the minimum and maximum values of the  $^8\text{B}$  fluxes anywhere within the designated allowed regions defined by the four free parameters.

The fluxes given in Table 2 are the total fluxes created at the sun and can therefore be directly compared with the predictions of the standard solar model. In terms of the best-estimate  $^8\text{B}$  neutrino flux from the BP2000 model ( $5.05 \times 10^8 \text{ cm}^2 \text{ s}^{-1}$ ), the total currently allowed range of solutions is, according to Table 2,

$$0.44 \leq \phi(^8B)_{\nu\text{-analysis}}/\phi(^8B)_{\text{BP2000}} \leq 1.95. \quad (2.1)$$

The corresponding  $3\sigma$  range allowed by the error analysis of the standard solar model is

$$0.52 \leq \phi(^8B)/\phi(^8B)_{\text{BP2000}} \leq 1.6. \quad (2.2)$$

The range allowed by the global analysis of neutrino experiments is slightly larger than the estimated  $3\sigma$  uncertainties in the standard solar model  $^8\text{B}$  neutrino flux pre-



diction. The largest allowed value of the  ${}^8\text{B}$  flux corresponds to neutrino parameters within the LMA allowed domain and the smallest allowed value is realized within the Just So<sup>2</sup> solution. The allowed range of the *hep* flux is

$$0.0 \leq \phi(\text{hep})_{\nu\text{-analysis}}/\phi(\text{hep})_{\text{BP2000}} \leq 12.0. \quad (2.3)$$

Because the uncertainty in the nuclear fusion cross section for the *hep* reaction is large and difficult to quantify, no estimated error is given for the *hep* neutrino flux in the standard solar model.

## 2.2 Computational method

We calculate the global  $\chi^2(f_B) = \chi_R^2(f_B) + \chi_{Sp}^2(f_B)$ , where the subscripts “*R*” and “*Sp*” stand for “Rates” and “Spectrum”, for each  $\Delta m^2$  and  $\tan^2 \theta$  on a  $201 \times 500$  lattice using 50 points per decade in both  $\tan^2 \theta$  and  $\Delta m^2$ . The validity of the  $\chi^2$  approach in this context, and some results of alternative approaches, are discussed in refs. [26, 27]. The parameter  $\Delta m^2$  varies from  $10^{-12}\text{eV}^2$  to  $10^{-3}\text{eV}^2$  and  $\tan^2 \theta$  varies from  $10^{-4}$  to  $10^1$ . The  ${}^8\text{B}$  neutrino flux is treated as a free parameter and at each step of the minimization process is kept the same in both individual  $\chi^2$ 's for the rates and for the spectrum. The  $\chi_R^2$  for the rates is calculated using the prescription given in [28], with updated uncertainties for the astrophysical parameters taken from BP2000 [23]. We do not include uncertainties in the  ${}^8\text{B}$  flux since we treat this flux as a free parameter.

For the calculation of  $\chi_{Sp}^2$ , we use the separate day and night spectra measured by the Super-Kamiokande collaboration and presented at Neutrino 2000 [29]. The statistical and systematic errors in the spectrum data are included as explained in [17] with the simple but important refinement of including separately the correlated and uncorrelated systematic errors in the off-diagonal and diagonal elements of the covariance matrix. We use the undistorted spectrum shape for  ${}^8\text{B}$  neutrinos that is given in ref. [30] (see also the very similar spectral shape of ref. [31]).

After the global  $\chi_{min}^2$  is determined, we draw the C.L. contours in the plane  $\tan^2 \theta - \Delta m^2$  by connecting points with equal  $\chi^2 = \chi_{min}^2 + \Delta\chi^2$ , where  $\Delta\chi^2 = 4.605, 5.99, 9.21, 11.83$  for 90, 95, 99 and 99.73 % C.L. for two degrees of freedom (the neutrino parameter  $\tan^2 \theta$  and  $\Delta m^2$ ).

For oscillations into an active neutrino, the survival probabilities for electron neutrinos produced in the Sun to arrive in the detector as an electron neutrino are calculated using the electron number density,  $n_e$ , in the BP2000 model [23]. For oscillations into sterile neutrinos, we use the effective density  $n_{\text{sterile}} = n_e - n_n/2$ , where  $n_n$  is the number density of neutrons in the BP2000 model [23]. We calculate numerically the survival probabilities, using a hybrid algorithm in which different approaches are used for different values of the parameter  $E/\Delta m^2$ .

For  $E/\Delta m^2 < 3 \times 10^6 \text{ MeV/eV}^2$  and all angles (including  $\theta > \pi/4$  [32, 21]), we use the well known analytical prescription [33] for calculating the survival probability at the surface of the Sun using the exact analytical solution for exponential density profiles [34, 35, 36]. The survival probability was averaged over the relevant production region for each neutrino flux (e. g.,  $^8\text{B}$  or  $^7\text{Be}$ ) as given in the BP2000 model [23].

For all other cases ( $E/\Delta m^2 > 3 \times 10^6 \text{ MeV/eV}^2$ ), first the transition probability  $P_{\odot}(\nu_e \rightarrow \nu_1)$  of an electron neutrino to the  $\nu_1$  neutrino mass eigenstate at the surface of the Sun was obtained numerically by solving the system of evolution equations in the form given in [37]. The same system of equations was used to calculate the transition probability  $P_{\oplus}(\nu_1 \rightarrow \nu_e)$  in the earth. The final survival probability was obtained using the formula [38]:

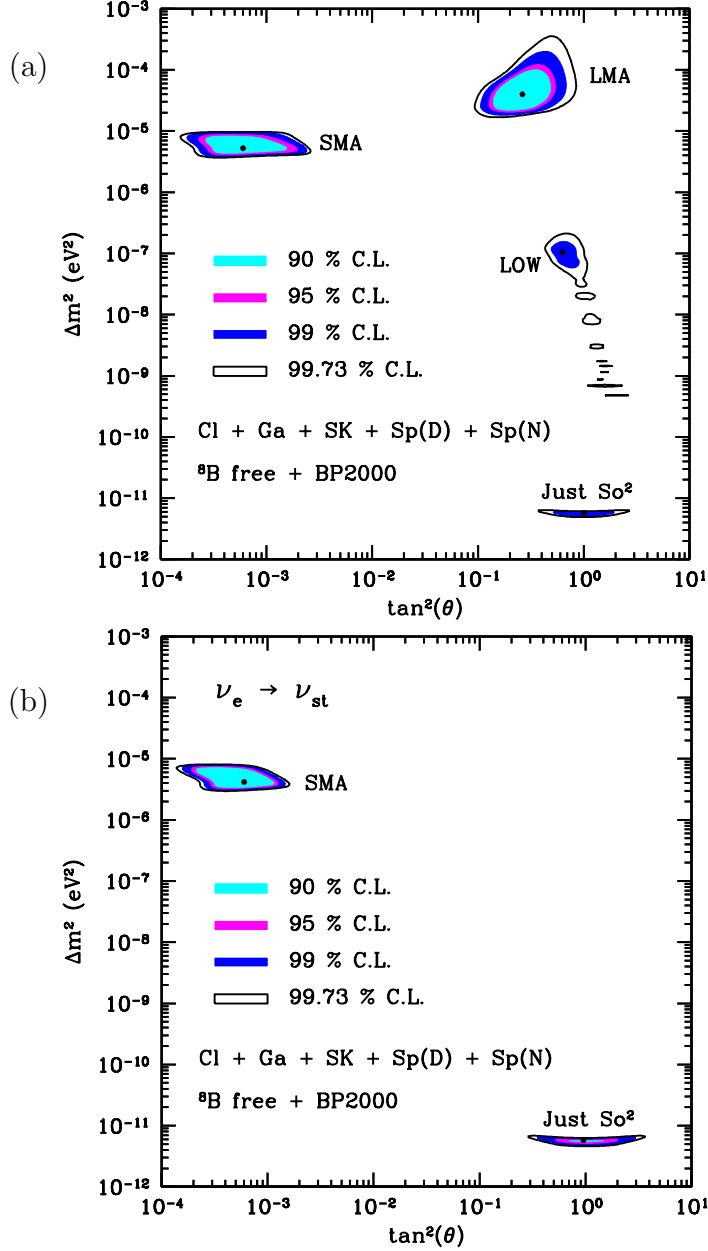
$$\begin{aligned}
P(\nu_e \rightarrow \nu_e) = & \\
& P_{\odot}(\nu_e \rightarrow \nu_1)P_{\oplus}(\nu_1 \rightarrow \nu_e) + (1 - P_{\odot}(\nu_e \rightarrow \nu_1))(1 - P_{\oplus}(\nu_1 \rightarrow \nu_e)) + \\
& 2\sqrt{P_{\odot}(\nu_e \rightarrow \nu_1)P_{\oplus}(\nu_1 \rightarrow \nu_e)(1 - P_{\odot}(\nu_e \rightarrow \nu_1))(1 - P_{\oplus}(\nu_1 \rightarrow \nu_e))} \cos \phi,
\end{aligned}
\tag{2.4}$$

where  $P_{\odot}(\nu_e \rightarrow \nu_1)$  is the transition probability that a  $\nu_e$  in the solar interior becomes a  $\nu_1$  mass eigenstate at the solar surface, and where  $P_{\oplus}(\nu_1 \rightarrow \nu_e)$  is the transition probability that a  $\nu_1$  becomes a  $\nu_e$  after crossing the earth. The quantity  $\phi$  is the phase difference of the amplitudes of the  $\nu_e \rightarrow \nu_1 \rightarrow \nu_e$  and  $\nu_e \rightarrow \nu_2 \rightarrow \nu_e$  transitions; the phase difference is acquired as the neutrino states propagate between the center of the Sun and the detector on Earth. The phase is calculated numerically at each stage of the propagation of the neutrino. In the region of parameter space where  $E/\Delta m^2 > 3 \times 10^6 \text{ MeV/eV}^2$ , averaging over the production region is unnecessary since the transitions take place far from the region of production.

The Earth regeneration effect is relevant for a rather limited range of  $E/\Delta m^2$ , which is:  $10^5 \text{ MeV/eV}^2 < E/\Delta m^2 < 10^8 \text{ MeV/eV}^2$ . In this region of parameter space we use the numerical procedure described in detail in ref. [25]. We calculate the transition probabilities along a number of trajectories (we use 0.5 degree spacing between adjacent trajectories) and average them for each detector by using accurately calculated weights proportional to the time the sun spends at different angles during the course of a year.

After the neutrinos leave the Sun and before they reach the detector, they oscillate in vacuum. The vacuum oscillations can be averaged over energy analytically for all relevant  $E/\Delta m^2$ , except for oscillation lengths comparable to or larger than about 1 A.U. Seasonal effects can be important for these longer oscillation lengths. The analytical formula for an exponential density profile already includes this averaging

**Figure 3:** Global solutions including Super-Kamiokande rate and with free  ${}^8\text{B}$  and  ${}_{\text{hep}}$  fluxes. (a) Active neutrinos. (b) Sterile neutrinos. The input data include the total rates measured in the Homestake, SAGE, GALLEX + GNO, and Super-Kamiokande experiments and the electron recoil energy spectrum measured by Super-Kamiokande during the day and also the spectrum measured at night. The best-fit points are marked by dark circles; the allowed regions are shown at 90%, 95%, 99%, and 99.73% C.L. .



over vacuum oscillations and no additional averaging is necessary when using this formula. In the region where the survival probabilities are calculated numerically, the averaging is done by propagating the neutrino state in vacuum over one oscillation length and then taking the average of the periodic survival probability over

the same distance. Since the equations describing neutrino oscillations in vacuum are exactly solvable, we use a simple analytical expression for the average survival probability. In the region  $E/\Delta m^2 > 5 \times 10^8 \text{MeV}/\text{eV}^2$ , we include the oscillations in vacuum using the one year averaged survival probabilities for which a convenient analytical expression exists [39].

### 3. Variations on a theme

In this section, we illustrate the extent to which the allowed oscillation regions are robust or fragile by performing the global analysis in different ways that have been used in the literature.

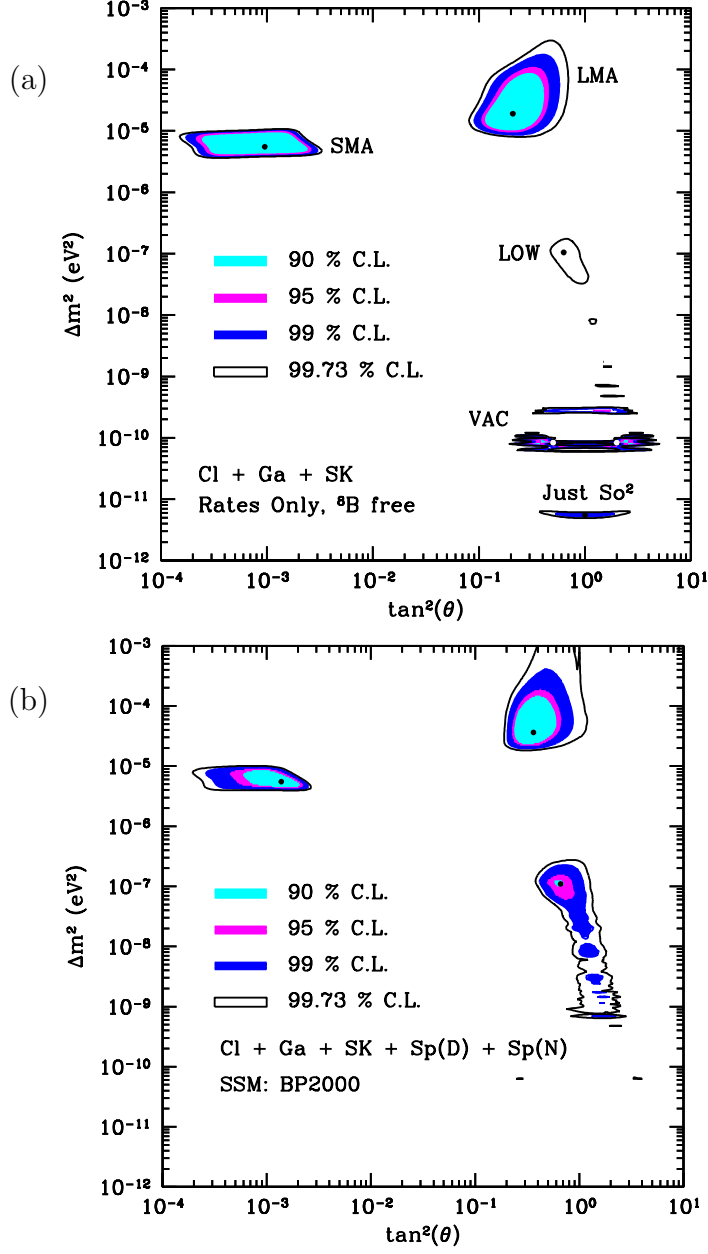
We do not repeat here a misleading procedure that has sometimes been used in the literature. It is incorrect to apply an exclusion region at a fixed confidence level based upon the results of a particular measured quantity (for example spectral data or day-night data) to an allowed region based upon consistency with other measured quantities (e. g., total rates). All of the measured quantities should be analyzed together in a single global fit, which is the procedure we follow in this paper.

Figure 3 presents the global solution for the case in which the Super-Kamiokande total rate is included together with the recoil electron energy spectrum. This double-counting procedure has been adopted in many analyses in the literature, including analyses that we have published. It would be correct to use both the total rate and the rates in each spectral bin if the total rate could be determined in a way that was independent of the spectral measurements. Since this is not the case [40], we have chosen as our standard analysis in this paper the results shown in Figure 1 in which only the spectral data are used for Super-Kamiokande.

Comparing Figure 1 and Figure 3, we see that the six most probable allowed regions (LMA, SMA, LOW, and Just So<sup>2</sup> for active neutrinos and SMA and Just So<sup>2</sup> for sterile neutrinos, cf. Table 1) are essentially unaffected by whether or not one includes the Super-Kamiokande total rate in the global analysis. The only qualitative change is that the least probable solutions in Figure 1, the vacuum solutions at  $\Delta m^2 \sim 10^{-10} \text{eV}^2$ , are absent if one includes the Super-Kamiokande rate.

Figure 4 illustrates how two different constraints affect the global solutions. The vacuum solutions with  $\Delta m^2 \sim 10^{-10} \text{eV}^2$  are prominent in Figure 4a, which was constructed in the same way as Figure 3a except that for Figure 4a only total rates, no spectral data, were considered. Comparing Figure 3a and Figure 4a, we see clearly that the spectral data have removed the previously prominent vacuum solutions. The symmetric best-fit points of the vacuum solution are marked by open circles in Figure 4a.

The only difference between the calculations that led to to Figure 4b and to Figure 3a is that for Figure 3a the BP2000 uncertainty for the <sup>8</sup>B neutrino flux was included in evaluating the contribution to the total  $\chi^2$  of the individual rates. The



**Figure 4:** Influence of constraints on global solutions. (a) Rates only, <sup>8</sup>B flux free. (b) <sup>8</sup>B flux constrained by BP2000 uncertainty. The calculations are the same as for Figure 3a except for one difference per panel. For Figure 4a, only total rates were considered and for Figure 4b, the total <sup>8</sup>B flux was constrained by the BP2000 standard solar model uncertainty in calculating the contribution of the rates to the total  $\chi^2$  but was allowed to vary to fit the spectrum.

imposition of the SSM flux constraint decreases somewhat the goodness of fit of the solutions. The best-fit points are shifted and the allowed regions are distorted.

Also, including the standard solar model constraints causes the LMA allowed region to overlap maximal mixing and to extend to larger  $\Delta m^2$  values (up to the region excluded by reactor experiments, see the upper right corner of Figure 4b).

Most dramatically, constraining the  ${}^8\text{B}$  neutrino flux while comparing the predictions to the total rates, eliminates the Just  $\text{So}^2$  solution from Figure 4b.

We conclude that the LMA, SMA, and LOW solutions for active neutrinos, and the SMA solution for sterile neutrinos, are all relatively robust. They have been present since the first global analysis that included Super-Kamiokande spectral and day-night data as well as the total rates in the radiochemical experiments [17].

The vacuum solutions at  $\Delta m^2 \sim 10^{-10}$  eV<sup>2</sup>, on the other hand, are relatively fragile. Whether or not the vacuum solutions are allowed depends upon how much one emphasizes the Super-Kamiokande data in the theoretical analysis. The vacuum solutions are present very prominently in the analysis if only the total rates are considered (see Figure 4a and ref. [17]), barely present if one includes the spectra data but not the total Super-Kamiokande rate (see Figure 1), and absent if one includes both the Super-Kamiokande rate and spectral data (see Figure 3).

The Just  $\text{So}^2$  solutions, vacuum and sterile, are allowed if one treats the  ${}^8\text{B}$  neutrino flux consistently as a free parameter in fitting both the total rates and the Super-Kamiokande spectral data.

## 4. Just $\text{So}^2$ Solution

Figure 1 contains two solutions, one for active neutrinos and one for sterile neutrinos, that only appear if the  ${}^8\text{B}$  flux is allowed to vary freely, namely, the solutions labeled “Just  $\text{So}^2$ .” These solutions correspond to a best-fit mixing angle of  $\theta = \pi/4$  and a very small squared mass difference of  $\Delta m^2 \sim 6 \times 10^{-12}$  eV<sup>2</sup> (cf. Table 1). At the end of this section, we discuss briefly the history of the Just  $\text{So}^2$  solutions [41, 42] and why they are not present in most analyses.

Figure 5 compares the Just  $\text{So}^2$  survival probability with the principal features of the solar neutrino spectrum, namely, the two most important continuum fluxes ( $p-p$  and  ${}^8\text{B}$ ) and the  ${}^7\text{Be}$  and  $pep$  neutrino lines. The line fluxes are expressed in units of  $10^{10}$  cm<sup>-2</sup> s<sup>-1</sup>. The continuum fluxes have the correct energy dependence but are multiplied by different constants, so that all the fluxes will fit conveniently onto the same figure with a linear vertical scale.

The reason for using the name Just  $\text{So}^2$  is apparent from Figure 5. The value of  $\Delta m^2$  is just such that the  ${}^7\text{Be}$  (0.86 MeV)  $\nu_e$  survival probability is very small ( $\sim 10\%$ ) and the  $\nu_e$  survival probability at the peak (0.31 MeV) of the  $p-p$  spectrum is very large ( $\sim 87\%$ ).

Neutrino Source	Cl (SNU)	Ga (SNU)
$p - p$	—	55.7
$pep$	0.1	1.6
${}^7\text{Be}$	0.1	5.1
${}^8\text{B}$	2.7	5.6
${}^{13}\text{N}$	0.02	0.7
${}^{15}\text{O}$	0.16	2.2
Total	3.1	70.9
Observed	$2.56 \pm 0.21$	$74.7 \pm 5.1$

**Table 3: Just So<sup>2</sup> solution.** The table lists, for the best-fit Just So<sup>2</sup> solution, the contribution of each flux to the chlorine and gallium experiments.

Figure 5 provides an intuitive way of understanding all the available solar neutrino experimental results. The lack of spectral energy distortion measured by Super-Kamiokande above 5 MeV is a direct result of the smallness of the assumed  $\Delta m^2$ ; practically no oscillations occur above 5 MeV. There is no predicted measurable day-night effect because matter effects are all negligible at such a small  $\Delta m^2$ . The SAGE and GALLEX plus GNO results are accounted for by having the  ${}^7\text{Be}$   $\nu_e$  flux almost entirely absent while the  $p - p$   $\nu_e$  flux is hardly diminished. The difference in the ratio of the predicted standard rate to the measured rate in the chlorine experiment (where it is a factor of three) and the Super-Kamiokande experiment (where

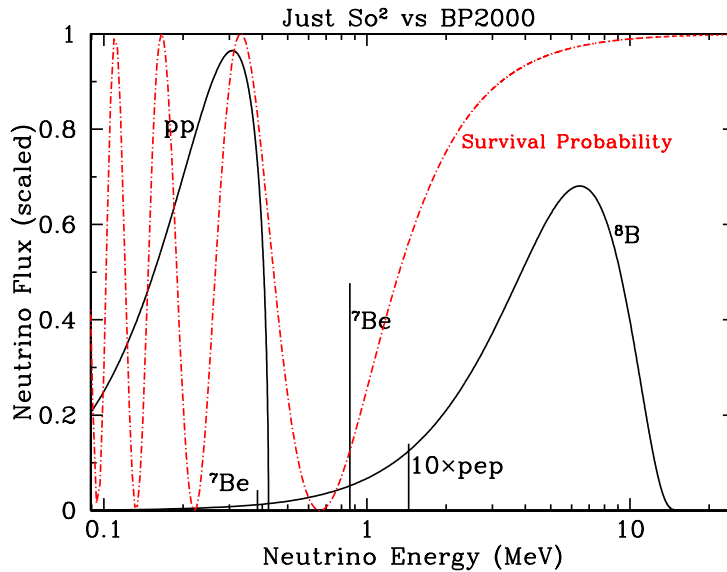


**Figure 5: Just So<sup>2</sup> vs BP2000.** The survival probability for the best-fit Just So<sup>2</sup> solution (dot-dashed line) is shown versus the scaled neutrino fluxes (continuous lines) predicted by the BP2000 solar model. The shapes of the continuous neutrino energy spectra are correct but the fluxes have been scaled by constant values in order to fit conveniently onto the same linear figure. The relative intensities of the  ${}^7\text{Be}$  and  $p - p$  lines are the same as in the BP2000 model.

it is a factor of two) is explained by the almost complete disappearance of the  ${}^7\text{Be}$  contribution to the chlorine experiment.

Table 3 gives the contributions of the individual neutrino fluxes to the chlorine and gallium experiments. The Just So<sup>2</sup> solution does not provide an excellent fit to the chlorine rate, but does provide very good fits to the rates of the gallium and Super-Kamiokande experiments. For Super-Kamiokande, the Just So<sup>2</sup> solution predicts a rate that is 0.461 of the standard model rate, in good agreement with the measured value [6] of  $0.475 \pm 0.016$ .

The Just-so<sup>2</sup> solution is allowed for both active and sterile neutrinos, with similar oscillation parameters and goodness of fit. In general, the difference between active and sterile solutions is due to the  $\nu_\mu$  and  $\nu_\tau$  that result from  $\nu_e$  conversion. The  $\nu_\mu$  and  $\nu_\tau$  can contribute to  $\nu - e$  scattering in SuperKamiokande. For the Just-So<sup>2</sup> solution, the oscillation effect is practically absent at energies for which SuperKamiokande is sensitive and therefore the  $\nu_\mu$  and  $\nu_\tau$  fluxes do not contribute significantly even for active neutrinos. This is the reason that for the experiments performed so far (but not for BOREXINO), there is no appreciable difference between the active and sterile cases for the Just So<sup>2</sup> solution.

Glashow and Krauss [43] proposed the name of ‘Just So’ neutrino oscillations to describe vacuum oscillations for a neutrino mass difference of  $\Delta m^2 = (50 - 130) \times 10^{-12} \text{ eV}^2$ . The mass of  $\Delta m^2$  was chosen by Glashow and Krauss so as to greatly reduce the  ${}^8\text{B}$  contribution to the chlorine experiment, assuming the validity of the standard solar model. For the Just So<sup>2</sup> solution considered here, the  ${}^8\text{B}$  flux is assumed, when produced at the sun, to already be significantly lower than predicted by the best standard solar model. The best-fit value of  $\Delta m^2 \sim 6 \times 10^{-12} \text{ eV}^2$  suppresses strongly the contribution of the  ${}^7\text{Be}$  neutrinos to the chlorine and gallium experiments, but (unlike the Glashow-Krauss solution) does not affect the small  ${}^8\text{B}$  flux assumed to be produced at the sun.

The Just So<sup>2</sup> solution was first found by Raghavan [41] and discovered independently and first analyzed in detail by Krastev and Petcov [42], who allowed the  ${}^8\text{B}$  flux to vary and compared the results with the total rates measured in the chlorine, Kamiokande, and gallium experiments (see also ref. [44]). No spectral data or day-night effects were available when this analysis was performed. The reason that the Just So<sup>2</sup> solution was not found in subsequent global solutions that included Super-Kamiokande spectral data is that for Just So<sup>2</sup> the  ${}^8\text{B}$  flux is  $3.3\sigma$  below the standard solar model [23] flux. In many previous global analyses, the  ${}^8\text{B}$  flux was allowed to vary in fitting the spectral data but was constrained by the standard model uncertainties in fitting the rate data [45, 46]. The Just So<sup>2</sup> solution does appear in Figure 8 of our analysis [17] with a free  ${}^8\text{B}$  flux of the total rates in the chlorine, gallium, and Super-Kamiokande experiments, but was not found in the same work when spectral and day-night data were included and the  ${}^8\text{B}$  flux was constrained by the standard solar model uncertainty.



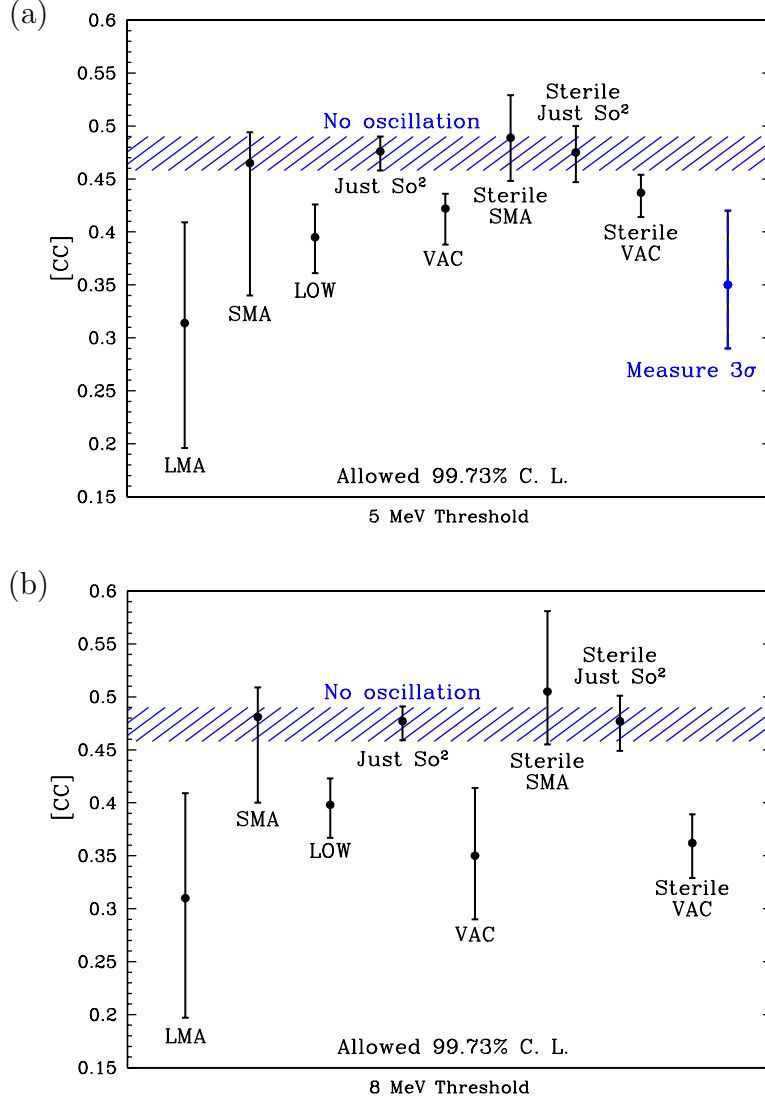


**Figure 6:** Comparison of the CC SNO rate and the no oscillation prediction. The shaded area is the no oscillation prediction based upon the measured Super-Kamiokande rate for  $\nu - e$  scattering. The SNO CC ratios,  $[CC] = (\text{to be measured})/(\text{BP2000})$ , are shown on the vertical axes for different neutrino scenarios and two different total electron energy thresholds, 5 MeV and 8 MeV. The error bars on the neutrino oscillation results represent the range of values predicted by the 99.73% CL allowed neutrino oscillation solutions displayed in Fig. 1.

## 5. Implications for the SNO experiment

In this section, we first discuss the predictions for the charged-current current rate in SNO and then discuss the predictions for the ratio of the neutral-current rate to

the charged-current rate. We use the solutions that are allowed at 99.73% C. L. in the global fit that is shown in Figure 1. We adopt in this section the notation of refs. [45, 47].

### 5.1 Predictions for the charged-current rate

The allowed range of neutrino parameters shown in Figure 1 corresponds to a range of predicted values for  $[\text{CC}]_{\text{SNO}}$ , the to-be-measured SNO charged-current rate divided by the predicted standard model rate for SNO charged-current reactions.

Figure 6 shows for each of the oscillation solutions the predicted range allowed at a nominal 99.7% C.L. . Since the predicted rate divided by the standard model rate depends upon the survival probability of solar  $\nu_e$ 's as a function of energy, the predicted values of  $[\text{CC}]_{\text{SNO}}$  depend upon the recoil electron energy threshold. Figure 6 gives results for both a 5 MeV threshold and an 8 MeV threshold. The dashed error bar labeled “Measure  $3\sigma$ ” represents the uncertainty in interpreting the measurements according to the best available estimates [47], which include the energy resolution, energy scale,  $^8\text{B}$  neutrino energy spectrum, neutrino cross section, and counting statistics (for one year of operation).

The numerical range for the  $[\text{CC}]$  ratio is, for a 5 MeV threshold: LMA (0.20 – 0.41), SMA (0.34 – 0.49), LOW (0.36 – 0.42), Just  $\text{So}^2$  (0.46 – 0.49), VAC (0.39 – 0.44) for active neutrinos and SMA (0.45 – 0.53), Just  $\text{So}^2$  (0.45 – 0.50) and VAC (0.41 – 0.45) for sterile neutrinos. For an 8 MeV threshold, we find for  $[\text{CC}]$ : LMA (0.20 – 0.41), SMA (0.40 – 0.51), LOW (0.36 – 0.42), Just  $\text{So}^2$  (0.46 – 0.49), VAC (0.29 – 0.41) for active neutrinos and SMA (0.45 – 0.58), Just  $\text{So}^2$  (0.45 – 0.50) and VAC (0.33 – 0.39) for sterile neutrinos.

For most of the currently allowed neutrino solution space, the predicted value of  $[\text{CC}]_{\text{SNO}}$  is expected to lie reasonably close to the non-oscillation value of  $[\text{CC}]_{\text{SNO}} = 0.475$ , which applies if neutrino oscillations do not occur and Super-Kamiokande is measuring a pure solar  $\nu_e$  beam. The SMA and Just  $\text{So}^2$  active neutrino solutions, as well as the SMA and Just  $\text{So}^2$  sterile neutrino solutions, all predict charged-current rates that are similar to the non-oscillation value. Only for certain LMA solution parameters is the predicted  $[\text{CC}]_{\text{SNO}}$  rate well separated from the Super-Kamiokande value.

The general trends shown in Figure 6 can be understood quantitatively by a simple relation that is easily derived:

$$[\text{CC}] = \frac{1}{1-r} \times [R_{\text{SK}} - r f_B] \times \frac{P_{\text{SNO}}}{P_{\text{SK}}}. \quad (5.1)$$

Here,  $R_{\text{SK}}$  is the ratio (0.475) of the neutrino-electron scattering rate observed by Super-Kamiokande to the rate expected on the basis of the standard solar model,  $r \sim 0.16$  is the ratio of neutrino-electron scattering cross sections for muon and electron neutrinos, and  $f_B$  is the ratio of the total  $^8\text{B}$  neutrino flux to the standard solar model

flux. The average survival probabilities,  $P_{\text{SNO}}$  and  $P_{\text{SK}}$ , refer to the energy ranges most important for the SNO and the Super-Kamiokande measurements. Equation 5.1 is valid for solutions like the LMA and LOW solutions (and somewhat less precisely for the SMA solution) in which the survival probability is practically constant over the region of interest. For the LMA and LOW solutions  $P_{\text{SNO}}/P_{\text{SK}} \approx 1$  independent of energy thresholds. The derivation of Equation 5.1 neglects the small energy-dependence of  $r$ .

In addition to providing insight into the trends shown in Figure 6, Equation 5.1 can be used to make ‘sanity-checks’ of detailed numerical calculations. The reader can make consistency checks of the results presented in Figure 6 by using the data given in Table 1 and Table 2.

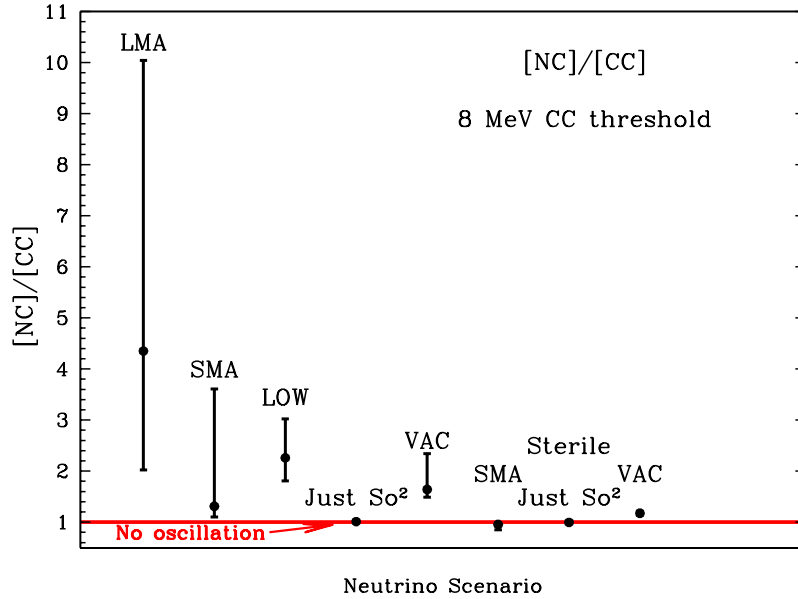
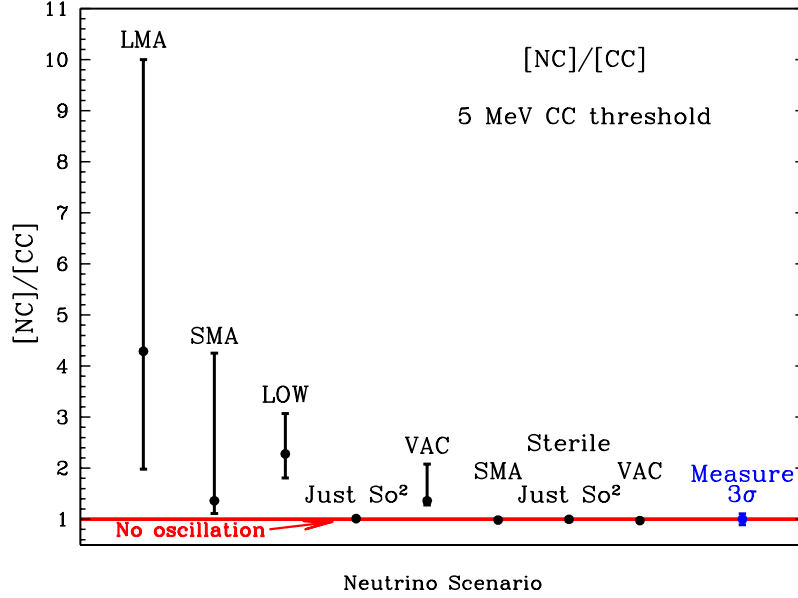
## 5.2 The ratio of neutral-current rate to charged-current rate

Figure 7 shows the predicted values of the double ratio,  $[\text{NC}]/[\text{CC}]$ . Here  $[\text{NC}]/[\text{CC}]$  is the ratio of the observed neutral-current rate to the charged-current rate in SNO divided by the same ratio calculated with the undistorted BP2000 fluxes. The standard model value for  $[\text{NC}]/[\text{CC}]$  is 1.0. Figure 7a shows, for a 5 MeV threshold for the CC measurement, the predicted double ratio of neutral-current to charged-current for the currently allowed neutrino oscillation scenarios. Figure 7b shows the same ratio but for an 8 MeV CC threshold. The solid error bars shown represent the 99.73% C.L. for the allowed regions of the six currently favored neutrino oscillation solutions in Figure 1. The error bar labeled “Measure  $3\sigma$ ” represents the uncertainty in interpreting the measurements according to the best available estimates [9, 47], which include the energy resolution, energy scale,  $^8\text{B}$  neutrino energy spectrum, neutrino cross section, and counting statistics (for 5000 CC events).

The numerical range for the ratio  $[\text{NC}]/[\text{CC}]$  is, for a 5 MeV CC threshold: LMA (2.0 – 10.0), SMA (1.1 – 4.0), LOW (1.8 – 3.1), Just  $\text{So}^2$  (1.011 – 1.016) for active neutrinos and SMA (0.964 – 0.997) and Just  $\text{So}^2$  (0.997 – 0.999) for sterile neutrinos. For an 8 MeV CC threshold, we find for  $[\text{NC}]/[\text{CC}]$ : LMA (2.05 – 10.05), SMA (1.1 – 3.4), LOW (1.8 – 3.0), Just  $\text{So}^2$  (1.008 – 1.013) for active neutrinos and SMA (0.89 – 0.99) and Just  $\text{So}^2$  (0.993 – 0.997) for sterile neutrinos.

The numerical range for the ratio  $[\text{NC}]/[\text{CC}]$  is, for a 5 MeV CC threshold: LMA (2.0 – 10.0), SMA (1.1 – 4.2), LOW (1.8 – 3.1), Just  $\text{So}^2$  (1.011 – 1.016) and VAC (1.3 – 2.1) for active neutrinos and SMA (0.952 – 0.996), Just  $\text{So}^2$  (0.997 – 0.999) and VAC (0.96 – 0.98) for sterile neutrinos. For an 8 MeV CC threshold, we find for  $[\text{NC}]/[\text{CC}]$ : LMA (2.0 – 10.0), SMA (1.1 – 3.6), LOW (1.8 – 3.0), Just  $\text{So}^2$  (1.008 – 1.012) and VAC (1.5 – 2.3) for active neutrinos and SMA (0.86 – 0.99), Just  $\text{So}^2$  (0.993 – 0.997) and VAC (1.13 – 1.21) for sterile neutrinos.

The LMA and LOW solutions are predicted to be well separated from the non-oscillation value of  $[\text{NC}]/[\text{CC}] = 1.0$ . However, the Just  $\text{So}^2$ , Sterile, and part of the SMA solution space are practically coincident with the no oscillation value.



**Figure 7:** The ratio of neutral-current rate to charged-current rate. Figure 7a shows, for a 5 MeV threshold for the CC measurement, the predicted double ratio of neutral-current rate to charged-current rate for different neutrino scenarios. Figure 7b shows the same ratio but for an 8 MeV CC threshold. The solid error bars shown represent the 99.73% C.L. for the allowed regions of the eight currently favored neutrino oscillation solutions in Figure 1. The first five solutions (from the left) refer to active neutrinos and the three following solutions refer to sterile neutrinos.

The most striking way that Figure 6 and Figure 7 differ from our previous results [47, 45] is that the Just So<sup>2</sup> are shown in the newer results. The fact that <sup>8</sup>B is treated as a free parameter in the present analysis both allows the Just So<sup>2</sup> solutions to appear and also decreases somewhat the predicted differences between the MSW active neutrino solutions and the no-oscillation expectations.

The trends in the double ratio can be represented by an analytic formula that is similar to, and derived in the same way, as Equation 5.1 and which uses the same notation:

$$\frac{[NC]}{[CC]} = \frac{f_B(1-r)}{[R_{SK} - rf_B]} \frac{P_{SK}}{P_{SNO}}. \quad (5.2)$$

## 6. Discussion

For both active and for sterile neutrinos, we have obtained a global solution, shown in Figure 1, for the eight allowed regions of neutrino oscillation parameters.

We allow the <sup>8</sup>B and *hep* neutrino fluxes created in the sun to be free parameters, treating the fluxes consistently in both the fits to the recoil energy spectrum and to the total event rates. However, we updated input data from the BP2000 standard solar model including the production profiles of the different neutrino sources, the number density profiles for scatterers of active and of sterile neutrinos, as well as the calculated fluxes, and their uncertainties, for all the neutrino fluxes except the <sup>8</sup>B and *hep* fluxes. So, our analysis is only a modest first step toward studying neutrino oscillations independently of solar models. More experimental data are required before one can begin to make studies of solar neutrinos that are truly independent of solar models.

Six of the currently allowed regions are robustly allowed, i. e., the LMA, SMA, LOW, and Just So<sup>2</sup> solutions for active neutrinos and the SMA and Just So<sup>2</sup> solutions for sterile neutrinos, are essentially unaffected by making common variations in the theoretical analysis. The vacuum solutions at  $\Delta m^2 \sim 10^{-10}$  eV<sup>2</sup> are rather fragile; whether or not they are present depends upon how strongly one emphasizes the Super-Kamiokande spectral energy data (see Section 3).

The Just So<sup>2</sup> solution with  $\Delta m^2 \sim 6 \times 10^{-12}$  eV<sup>2</sup> is allowed in the present analysis because we treat the <sup>8</sup>B flux as a free parameter in fitting both the spectral and the total rate data. The total <sup>8</sup>B neutrino flux required for the Just So<sup>2</sup> solution is 3.3 $\sigma$  below the best-estimate <sup>8</sup>B flux of the standard solar model, using both the flux and the uncertainty of the BP2000 model.

The Just So<sup>2</sup> solution, discussed in Section 4 and in refs. [41, 42] and illustrated in Figure 5, describes in an obvious way all of the solar neutrino results measured so far. One can see immediately from Figure 5 that the predicted distortion of the <sup>8</sup>B neutrino spectrum is very small in the region accessible to Super-Kamiokande and SNO (above 5 MeV). The day-night effect is predicted to be zero. The rates

measured in the radiochemical experiments, chlorine and gallium, are accounted for by the strongly suppressed  ${}^7\text{Be}$   $\nu_e$  flux, the only slightly suppressed  $p-p$   $\nu_e$  flux ( $\sim 23\%$  for the gallium experiments), and the inferred relatively low total  ${}^8\text{B}$  neutrino flux, 0.47 of the BP2000 value.

Unfortunately, the Just  $\text{So}^2$  solution will not be distinguishable by SNO from the no oscillation hypothesis (see Figure 6 and Figure 7). BOREXINO and other experiments with sensitivity below 1 MeV will be required to identify Just  $\text{So}^2$  oscillations if Nature has chosen this simple but elusive solution.

Figure 6 shows that the [CC] measurement by SNO will not reveal strong evidence for neutrino oscillations unless Nature has chosen a favorable part of the currently allowed LMA oscillation space (cf. Figure 1). The predictions for [CC] based upon the best-fit parameters of four solutions, the active and sterile SMA solutions and the active and sterile Just  $\text{So}^2$  solutions, all lie within the no-oscillation band illustrated in Figure 6. The fragile vacuum solutions with  $\Delta m^2 \sim 10^{-10} \text{ eV}^2$  both lie close to the no-oscillation band. Of the eight solutions illustrated in Figure 6, only the LMA solution offers the possibility of a definitive ( $> 3\sigma$ ) deviation from the no-oscillation hypothesis.

The diagnostic power of the ratio of neutral-current rate to charged-current rate,  $[\text{NC}]/[\text{CC}]$ , is much greater. The current best global solution predicts a significant deviation from the no-oscillation hypothesis if either of the LMA, SMA, LOW or VAC solutions for active neutrinos is valid. But the Just  $\text{So}^2$  active neutrino solution and the Just  $\text{So}^2$  and SMA sterile neutrino solutions predict a double ratio that can be consistent with the no-oscillation value. The predicted numerical range for the  $[\text{NC}]/[\text{CC}]$  ratio is given in Section 5 for each of the currently allowed oscillation regions.

JNB and PIK acknowledge support from NSF grant No. PHY0070928 and PIK acknowledges support from DOE grant DE-FG02-84ER40163. We are grateful to A. Friedland and E. Lisi for valuable comments and suggestions.

## References

- [1] R. Davis, Jr., D.S. Harmer and K.C. Hoffman, *Search for neutrinos from the sun*, *Phys. Rev. Lett.* **20** (1968) 1205.
- [2] J.N. Bahcall, N.A. Bahcall and G. Shaviv, *Present status of the theoretical predictions for the  ${}^{37}\text{Cl}$  solar-neutrino experiment*, *Phys. Rev. Lett.* **20** (1968) 1209.
- [3] Y. Fukuda et al. (Kamiokande Collaboration), *Solar neutrino data covering solar cycle 22*, *Phys. Rev. Lett.* **77** (1996) 1683.
- [4] J.N. Abdurashitov et al. (SAGE Collaboration), *Measurement of the solar neutrino capture rate with gallium metal*, *Phys. Rev.* **C 60** (1999) 055801; V. Gavrin (SAGE Collaboration), *Solar neutrino results from SAGE*, in *Neutrino 2000*, Proc. of the

- XIXth International Conference on Neutrino Physics and Astrophysics, 16–21 June 2000, eds. J. Law, R.W. Ollerhead, and J.J. Simpson, *Nucl. Phys.* **B 91** (Proc. Suppl.), 36.
- [5] W. Hampel et al. (GALLEX Collaboration), *GALLEX solar neutrino observations: results for GALLEX IV*, *Phys. Lett.* **B 447** (1999) 127.
- [6] Y. Fukuda et al. (Super-Kamiokande Collaboration), *Measurements of the solar neutrino flux from Super-Kamiokande's first 300 days*, *Phys. Rev. Lett.* **81** (1998) 1158; Erratum **81** (1998) 4279; *Constraints on neutrino oscillation parameters from the measurement of day-night solar neutrino fluxes at Super-Kamiokande*, *Phys. Rev. Lett.* **82** (1999) 1810; Y. Suzuki (Super-Kamiokande Collaboration), *Solar neutrino results from Super-Kamiokande*, in *Neutrino 2000*, Proc. of the XIXth International Conference on Neutrino Physics and Astrophysics, 16–21 June 2000, eds. J. Law, R.W. Ollerhead, and J.J. Simpson, *Nucl. Phys.* **B 91** (Proc. Suppl.), 29.
- [7] M. Altmann et al. (GNO Collaboration), *GNO solar neutrino observations: results for GNO I*, *Phys. Lett.* **B 490** (2000) 16; E. Bellotti et al. (GNO Collaboration), *First results from GNO*, in *Neutrino 2000*, Proc. of the XIXth International Conference on Neutrino Physics and Astrophysics, 16–21 June 2000, eds. J. Law, R.W. Ollerhead, and J.J. Simpson, *Nucl. Phys.* **B 91** (Proc. Suppl.), 44.
- [8] B.T. Cleveland et al., *Measurement of the solar electron neutrino flux with the Homestake chlorine detector*, *Astrophys. J.* **496** (1998) 505.
- [9] A.B. McDonald (SNO collaboration), *The Sudbury Neutrino Observatory project*, *Nucl. Phys.* **B 77** (Proc. Suppl.) (1999) 43; G.T. Ewan, W.F. Davidson and C.K. Hargrove (SNO Collaboration), *The Sudbury Neutrino Observatory—an introduction*, *Physics in Canada* **48** (1992) 112; SNO Collaboration, *The Sudbury Neutrino Observatory*, *Nucl. Instrum. Meth.* **A 449** (2000) 172.
- [10] G. Alimonti et al. (BOREXINO collaboration), *Science and Technology of BOREXINO: a real time detector for low energy solar neutrinos* [hep-ex/0012030].
- [11] P. Alivisatos et al. (the KamLAND collaboration), *The KamLAND proposal*, Stanford-HEP-98-03; A. Piepke (KamLAND Collaboration), *KamLAND: A reactor neutrino experiment testing the solar neutrino anomaly*, in *Neutrino 2000*, Proc. of the XIXth International Conference on Neutrino Physics and Astrophysics, 16–21 June 2000, eds. J. Law, R.W. Ollerhead and J.J. Simpson, *Nucl. Phys.* **B 91** (Proc. Suppl.), 99.
- [12] ICARUS collaboration, *Study of solar neutrinos with the 6 t liquid argon ICARUS detector*, *Nucl. Instr. and Methods* **A 455** (2000) 376.
- [13] V.N. Gribov and B.M. Pontecorvo, *Neutrino astronomy and lepton charge*, *Phys. Lett.* **B 28** (1969) 493; B. Pontecorvo, *Neutrino experiments and the problem of conservation of leptonic charge*, *Sov. Phys. JETP* **26** (1968) 984.

- [14] L. Wolfenstein, *Neutrino Oscillations in Matter*, *Phys. Rev.* **D 17** (1978) 2369; S.P. Mikheyev and A.Yu. Smirnov, *Resonance enhancement of oscillations in matter and solar neutrino spectroscopy*, *Yad. Fiz.* **42** (1985) 1441 [*Sov. J. Nucl. Phys.* **42** (1985) 913].
- [15] J.N. Bahcall, *Neutrino Astrophysics*, Cambridge University Press, Cambridge, 1989.
- [16] J.N. Bahcall, S. Basu and M.H. Pinsonneault, *How uncertain are solar neutrino predictions?*, *Phys. Lett.* **B 433** (1998) 1.
- [17] J.N. Bahcall, P.I. Krastev and A.Yu. Smirnov, *Where do we stand with solar neutrino Oscillations?*, *Phys. Rev.* **D 58** (1998) 096016.
- [18] G. L. Fogli, E. Lisi, and D. Montanino, *The solar neutrino problem after three hundred days of data at SuperKamiokande*, *Astropart. Phys.* **9** (1998) 119.
- [19] P.I. Krastev and A.Yu. Smirnov, *Boron neutrino flux and resonant conversion of solar neutrinos*, *Phys. Lett.* **B 338** (1994) 282; J.N. Bahcall and P.I. Krastev, *How well do we (and will we) know solar neutrino fluxes and oscillation parameters?*, *Phys. Rev.* **D 53** (1996) 4211; R. Barbieri, L.J. Hall, D. Smith, A. Strumia and N. Weiner, *Oscillations of solar and atmospheric neutrinos*, *JHEP* **12** (1998) 017; R. Barbieri and A. Strumia, *Non standard analysis of the solar neutrino anomaly*, *JHEP* **12** (2000) 016.
- [20] M.C. Gonzalez-Garcia, P.C. de Holanda, C. Pena-Garay and J.W.F. Valle, *Status of the MSW solutions to the solar neutrino problem*, *Nucl. Phys.* **B 573** (2000) 3.
- [21] A. Gouvea, A. Friedland and H. Murayama, *The dark side of the solar neutrino parameter space*, *Phys. Lett.* **B 490** (2000) 125.
- [22] M.C. Gonzalez-Garcia and C. Pena-Garay, *Global and unified analysis of solar neutrino data*, *Nucl. Phys., (Proc. Suppl.)* **B 91** (2000) 80; M.C. Gonzalez-Garcia, M. Maltoni, C. Pena-Garay and J.W.F. Valle, *Global three-neutrino oscillation analysis of neutrino data*, *Phys. Rev.* **D 63** (2001) 033005.
- [23] J.N. Bahcall, M.H. Pinsonneault and S. Basu, *Solar models: current epoch and time dependences, neutrinos, and heliosiesmological properties*, *Astrophys. J.* (accepted) [astro-ph/0010346].
- [24] G.L. Fogli, E. Lisi and D. Montanino, *Matter-enhanced three-flavor oscillations and the solar neutrino problem*, *Phys. Rev.* **D 54** (1996) 2048.
- [25] J.N. Bahcall and P.I. Krastev, *Does the sun appear brighter at night in neutrinos?*, *Phys. Rev.* **C 56** (1997) 2839.
- [26] M.V. Garzelli and C. Giunti *A frequentist analysis of solar neutrino data* [hep-ph/0007155]
- [27] P. Creminelli, G. Signorelli and Alessandro Strumia, *Frequentist analyses of solar neutrino data* [hep-ph/0102234].



- [28] G.L. Fogli and E. Lisi, *Standard solar model uncertainties and their correlations in the analysis of the solar neutrino problem*, *Astropart. Phys.* **3** (1995) 185.
- [29] Y. Suzuki and M. Smy, private communication.
- [30] J. N. Bahcall, E. Lisi, D.E. Alburger, L. De Braekeleer, and S. J. Freedman, *Phys. Rev.* **C54** (1996) 411.
- [31] C.E. Ortiz, A. Garcia, R.A. Waltz, M. Bhattacharya, and A.K. Komives, *Phys. Rev. Lett.* **85** (2000) 2909.
- [32] A. Friedland, *Mikheyev-Smirnov-Wolfenstein effects in vacuum oscillations*, *Phys. Rev. Lett.* **85** (2000) 936.
- [33] P.I. Krastev and S.T. Petcov, *On the analytic description of two-neutrino transitions of solar neutrinos in the sun*, *Phys. Lett.* **B 207** (1988) 64; Erratum **214** (1988) 661.
- [34] T. Kaneko, *Analytic solution for resonant mixing of solar neutrinos*, *Prog. Theor. Phys.* **78** (1987) 532; M. Ito, T. Kaneko and M. Nakagawa, *On analytic solution of resonant mixing for solar neutrino oscillations*, *Prog. Theor. Phys.* **79** (1988) 13; Erratum **79** (1988) 555.
- [35] S. Toshev, *Exact analytical solution of the two-neutrino evolution equation in matter with exponentially varying density*, *Phys. Lett.* **B 196** (1987) 170.
- [36] S.T. Petcov, *Exact analytic description of two-neutrino oscillations in matter with exponentially varying density*, *Phys. Lett.* **B 200** (1988) 373.
- [37] S.P. Mikheyev and A.Yu. Smirnov, *Resonant amplifications of  $\nu$ -oscillations in matter and solar-neutrino spectroscopy*, *Nuovo Cimento* **C 9** (1986) 17.
- [38] G.L. Fogli, E. Lisi, D. Montanino and A. Palazzo, *Quasivacuum solar neutrino oscillations*, *Phys. Rev.* **D 62** (2000) 113004.
- [39] B. Faid, G.L. Fogli, E. Lisi and D. Montanino, *Solar neutrinos: near-far asymmetry and just-so oscillations*, *Phys. Rev.* **D 55** (1997) 1353.
- [40] Y. Suzuki, 3/2001 (private communication).
- [41] R.S. Raghavan, *Solar neutrinos—from puzzle to paradox*, *Science* **267** (1995) 45.
- [42] P.I. Krastev and S.T. Petcov, *On the vacuum oscillation solutions of the solar neutrino problem*, *Phys. Rev.* **D 53** (1996) 1665.
- [43] S.L. Glashow and L.M. Krauss, *“Just so” neutrino oscillations*, *Phys. Lett.* **B 190** (1987) 199.
- [44] Q. Y. Liu and S. T. Petcov, *Three-Neutrino Mixing and Combined Vacuum Oscillations and MSW Transitions of Solar Neutrinos*, *Phys. Rev.* **D 56** (1997) 7392.

- [45] J.N. Bahcall, P.I. Krastev and A.Yu. Smirnov, *What will the first year of SNO show?*, *Phys. Lett. B* **477** (2000) 401.
- [46] G.L. Fogli, E. Lisi, D. Montanino and A. Palazzo, *Three-flavor MSW solutions of the solar neutrino problem*, *Phys. Rev. D* **62** (2000) 013002.
- [47] J.N. Bahcall, P.I. Krastev and A.Yu. Smirnov, *SNO: predictions for ten measurable quantities*, *Phys. Rev. D* **62** (2000) 93004.